European Polymer Journal 49 (2013) 3261–3270

Contents lists available at SciVerse ScienceDirect

European Polymer Journal

journal homepage: www.elsevier.com/locate/europolj

Conjugated polymer consisting of dibenzosilole and quinoxaline as donor materials for organic photovoltaics

Ho Jun Song, Joo Young Lee, Eui Jin Lee, Doo Kyung Moon *

Department of Materials Chemistry and Engineering, Konkuk University, 1 Hwayang-dong, Gwangjin-gu, Seoul 143-701, Republic of Korea

ARTICLE INFO

Article history:
Received 24 April 2013
Received in revised form 21 June 2013
Accepted 25 June 2013
Available online 4 July 2013

Keywords:
Dibenzosilole
Quinoxaline
OPVs
Conjugated polymer

ABSTRACT

The new D–A type polymers poly(dibenzosilole-diphenylquinoxaline) (PSiPDTQ) and dibenzosilole-dibenzophenazine) (PSiFDTQ), both of which adopted benzosilole as a donor, were polymerized through a Suzuki coupling reaction. PSiPDTQ and PSiFDTQ were able to be dissolved in organic solvents and exhibited high thermal stability. Due to the appropriate LUMO energy levels, an effective charge transport was observed in PSiPDTQ and PSiFDTQ. According to X-ray diffraction measurements, a single broad diffraction peak was detected at approximately 20.5°. The π–π stacking distances (d_π) for PSiPDTQ and PSiFDTQ were 4.4 and 4.3 Å, respectively. When PSiPDTQ and $PC_{71}BM$ were blended in a 1:3 ratio and used as the active layer in a solar cell, the resulting V_{oc}, J_{sc}, FF and PCE were 0.89 V, 5.1 mA/cm^2, 30.2% and 1.4%, respectively. For solar cells using a 1:6 ratio of PSiFDTQ to $PC_{71}BM$, the resulting V_{oc}, J_{sc}, FF and PCE were 0.98 V, 3 mA/cm^2, 52.8% and 1.6%, respectively. In addition, for a PSiPDTQ and $PC_{71}BM$ blended film (1:3 ratio) with an additional layer of PFN, the PCE of the resulting solar cells was improved (relative to solar cells without PFN) to 2.1% due to the interfacial adhesion of PFN.

1. Introduction

For several decades, semiconducting polymers have been used in diverse applications, such as organic light emitting diodes (OLEDs) [1–4], organic photovoltaic cells (OPVs) [5–11] and organic thin film transistors (OTFTs) [12,13]. Of these applications, OPVs have drawn great attention with the global technology trend toward economic feasibility and continuous development, while preserving the environment. Low power conversion efficiency (PCE) has been the largest obstacle to the development of OPVs [6]. Over the past few years, Donor–Acceptor (D–A) type low-band gap polymers have drawn great attention, as their electronic properties can be easily be changed based on the unique combination of the D–A unit. These polymers can also exhibit broader absorption spectra to longer wavelengths compared to more traditional polymers.

Among the D–A polymer acceptor units, the quinoxaline derivatives have been widely used due to the electron-withdrawing properties of the two imine nitrogens. The quinoxaline derivatives can be easily structurally deformed and exhibit high solubility. In addition, the quinoxaline derivatives exhibit electronic properties that can be changed with various substituents [14–18]. Recently, the Jen group reported that with the two phenyl rings connected to the single bond between the ortho-positions, the PCE of OPVs improved by 0.55% to achieve an efficiency of 6.24% [19]. These fused-phenyl rings can enhance the efficiency through a reduction of the energetic disorder of the polymer after facilitating polymer coplanarity and interchain π–π interactions. In these fused-phenyl rings, however, it is difficult to introduce the akyl-chains necessary to become highly soluble. Recently, we reported D–A polymers of quinoxaline and dibenzo-phenazine derivatives that introduced alkoxy-chains at the 6th, 7th or

* Corresponding author. Tel.: +82 2 450 3498; fax: +82 2 444 0765.
E-mail address: dkmoon@konkuk.ac.kr (D.K. Moon).

0014-3057/$ - see front matter © 2013 Elsevier Ltd. All rights reserved.
http://dx.doi.org/10.1016/j.eurpolymj.2013.06.032

11th, 12th positions [20]. These types of alkoxy-quinoxaline and dibenzo-phenazine derivatives exhibit a high solubility and maintain the absorption spectrum and electronic properties of quinoxaline. In particular, the polymer of the alkoxy-dibenzo-phenazine derivative exhibited effective intra-molecular charge transfer (ICT) and coplanar properties.

Recently, some copolymers that contain silicon atoms have already been reported in the literature [21–23], and have shown hole mobilities that rival those of polyfluorenes without any optimization of the polymer molecular weight and film deposition/processing conditions.

In this study, two new D–A type polymers, poly(dibenzosilole-diphenylquinoxaline) (PSiPDTQ) and poly(dibenzosilole-dibenzophenazine) (PSiFDTQ), in which dibenzosilole derivatives were introduced as a donor, were successfully polymerized. Compared with PSiPDTQ, a more effective π–π interaction is expected in PSiFDTQ because of the superior coplanarity properties of the fused-phenyl rings, which enables a high FF in OPVs.

2. Experimental section

2.1. Instruments and characterization

Unless otherwise specified, all reactions were performed under a nitrogen atmosphere. The solvents were dried using the standard procedures. All column chromatography was performed with silica gel (230–400 mesh, Merck) as the stationary phase. ^{1}H NMR spectra were collected by a Bruker ARX 400 spectrometer using solutions in $CDCl_3$ with chemical concentrations recorded in ppm units using TMS as the internal standard. The elemental analyses were measured with an EA1112 apparatus using a CE Instrument. The electronic absorption spectra were measured in chloroform using an HP Agilent 8453 UV–Vis spectrophotometer. The cyclic voltammetric waves were obtained using a Zahner IM6eX electrochemical workstation with a 0.1 M acetonitrile (purged with nitrogen for 20 min) solution containing tetrabutyl ammonium hexafluorophosphate (Bu_4NPF_6) as the electrolyte at a constant scan rate of 50 mV/s. ITO, a Pt wire, and silver/silver chloride [Ag in 0.1 M KCl] were used as the working, counter, and reference electrodes, respectively. The electrochemical potential was calibrated against Fc/Fc^+. The HOMO levels of the polymers were determined using the oxidation onset value. The onset potentials are the values obtained from the intersection of the two tangents drawn at the rising current and the baseline changing current of the CV curves. TGA measurements were performed on a NETZSCH TG 209 F3 thermogravimetric analyzer. All GPC analyses were performed using THF as an eluent and a polystyrene standard as a reference. X-ray diffraction (XRD) patterns were obtained using a SmartLab 3 kW (40 kV 30 mA, Cu target, wavelength: 1.541871 Å) instrument of Rigaku, Japan. Topographic images of the active layers were obtained through atomic force microscopy (AFM) in a tapping mode under ambient conditions using an XE-100 instrument. Theoretical analyses were performed using density functional theory (DFT), as approximated by the B3 LYP functional and employing the 6-31G* basis set in Gaussian09.

2.2. Fabrication and characterization of polymer solar cells

All of the bulk-heterojunction PV cells were prepared using the following device fabrication procedure. The glass/indium tin oxide (ITO) substrates [Sanyo, Japan (10 Ω/γ)] were sequentially lithographically patterned, cleaned with detergent, and ultrasonicated in deionized water, acetone, and isopropyl alcohol. The substrates were then dried on a hot plate at 120 °C for 10 min and treated with oxygen plasma for 10 min to improve the contact angle immediately before the film coating process. Poly(3,4-ethylene-dioxythiophene): poly(styrene-sulfonate) (PEDOT:PSS, Baytron P 4083 Bayer AG) was passed through a 0.45-μm filter before being deposited onto the ITO substrates at a thickness of ca. 32 nm by spin-coating at 4000 rpm in air and then dried at 120 °C for 20 min inside a glove box. Composite solutions with polymers and PCBM were prepared using chlorobenzene (CB) with 1,8-diiodooctane (DIO). The concentration was adequately controlled in the 0.3–0.5 wt% range. The solutions were then filtered through a 0.45-μm PTFE filter and spin-coated (500–2000 rpm, 30 s) on top of the PEDOT:PSS layer. The PFN solution in methanol and acetic acid was spin-coated on the top of the obtained active layer at 4000 rpm for 30 s to form a thin interlayer of 5 nm. The device fabrication was completed by depositing thin layers of Al (200 nm) at pressures of less than 10^{-6} torr. The active area of the devices was 4.0 mm^2. Finally, the cell was encapsulated using a UV-curing glue (Nagase, Japan). In this study, all of the devices were fabricated with the following structure: ITO glass/PEDOT:PSS/polymer:PCBM/PFN/Al/encapsulation glass.

The illumination intensity used to test the OPVs was calibrated using a standard a Si photodiode detector that was equipped with a KG-5filter. The output photocurrent was adjusted to match the photocurrent of the Si reference cell to obtain a power density of 100 mW/cm^2. After the encapsulation, all of the devices were operated under an ambient atmosphere at 25 °C. The current–voltage (I–V) curves of the photovoltaic devices were measured using a computer-controlled Keithley 2400 source measurement unit (SMU) that was equipped with a Peccell solar simulator under an illumination of AM 1.5G (100 mW/cm^2). The thicknesses of the thin films were measured using a KLA Tencor Alpha-step 500 surface profilometer with an accuracy of 1 nm.

2.3. Synthesis

All reagents were purchased from Aldrich, Acros or TCI companies. All chemicals were used without further purification. 5,5-dioctyl-3,7-bis(4,4,5,5-tetramethyl-1,3,2-dioxaborolan-2-yl)-5H-dibenzo[b,d]silole was purchased from Luminescence Technology Crop (Product NO.: B1181). The following compounds were synthesized following modified literature procedures: 5,8-bis(5-bromothiophen-2-yl)-6,-7-bis(octyloxy)-2,3-diphenylquinoxaline (M1), 10,13-bis(5- bromothiophen-2-yl)-11,12-bis(octyloxy)dibenzo [a,c]phenazine (M2) [20].

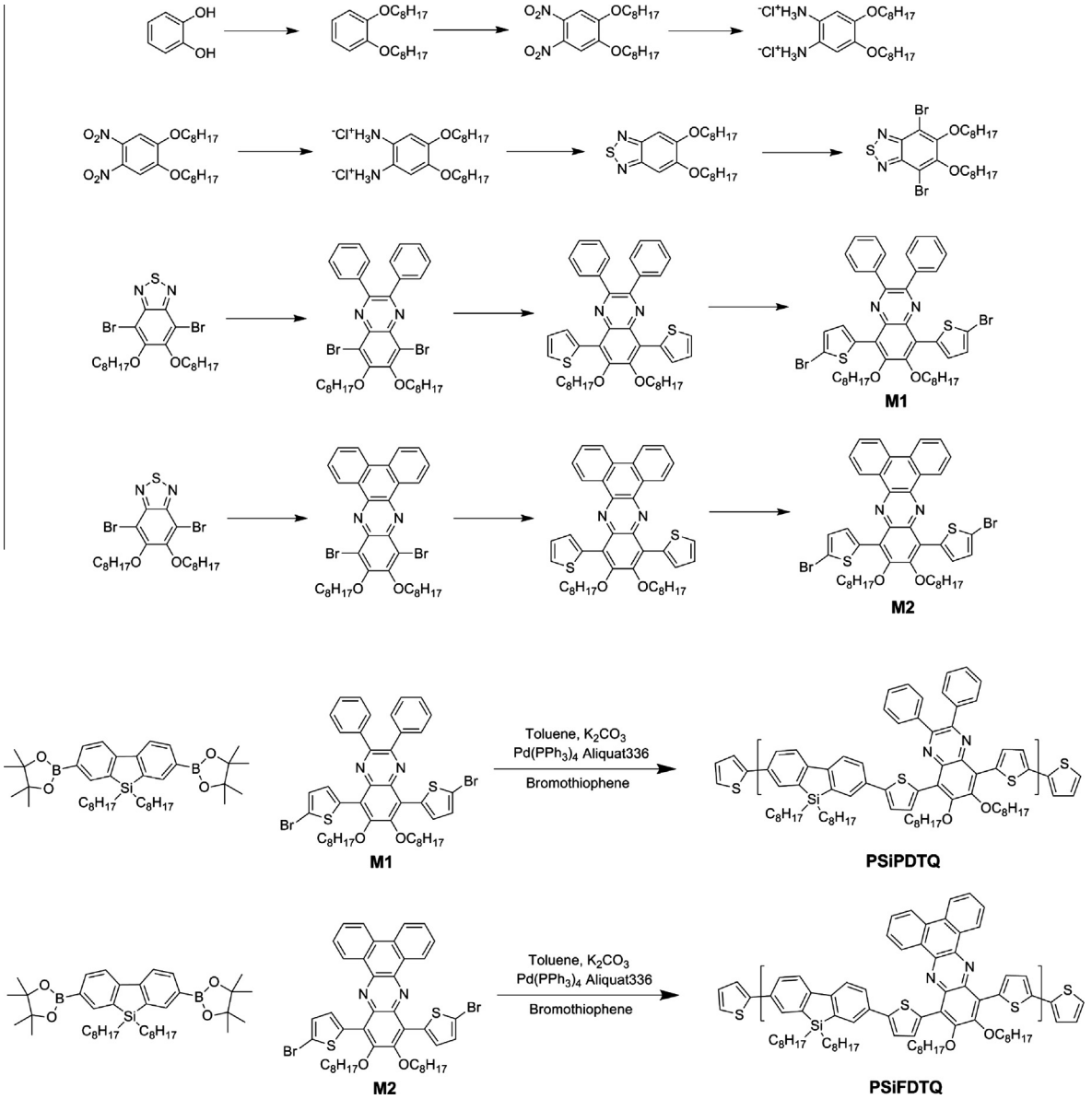

Scheme 1. Scheme of monomer synthesis and polymerization.

Table 1
Molecular weight and thermal properties of the polymers.

Polymer	M_n (kg/mol)	M_w (kg/mol)	PDI	T_d (°C)
PSiPDTQ	18.6	36.9	1.98	338
PSiFDTQ	16.5	35.7	2.16	332

2.4. Poly[dibenzosilole-alt-dithienyl-diphenylquinoxaline] (PSiPDTQ)

5,5-Dioctyl-3,7-bis(4,4,5,5-tetramethyl-1,3,2-dioxaborolan-2-yl)-5H-dibenzo[b,d]silole (0.15 g, 0.23 mmol), M1 (0.2 g, 0.23 mmol), $Pd(PPh_3)_4$(0) (0.008 g, 0.007 mmol) and Aliquat336, were placed in a Schlenk tube, purged with three nitrogen/vacuum cycles, and under a nitrogen atmosphere, added 2 M degassed aqueous K_2CO_3 (7 mL) and dry toluene (10 mL). The mixture was placed in a microwave reactor and heated to 90 °C using 300 W of microwave power for 20 min. After the polymerization was completed, the polymer was end-capped with bromothiophene. After reaction quenching, the entire mixture was poured into methanol. The precipitate was filtered off and purified with a Soxhlet extraction in the following order: methanol, acetone and chloroform. The polymer was recovered from the chloroform fraction and precipitated into methanol. The final product was obtained after drying in vacuum. Dark red solid (0.13 g 56%). ^{1}H NMR (400 MHz; $CDCl_3$; Me_4Si): δ = 8.19–8.10 (m), 7.82–7.69 (m), 7.57–7.38 (m), 4.17 (br, 4H), 1.90 (br,

4H), 1.53–1.23 (m), 0.90–0.64 (m). Anal. Calcd for: $C_{72}H_{90}N_2O_2S_2Si$: C, 78.07; H, 8.19; N, 2.53; O, 2.89; S, 5.79. Found: C, 76.25; H, 7.85; N, 2.53; O, 2.33; S, 5.85.

2.5. Poly[dibenzosilole-alt-dithienyl-dibenzophenazine] (PSiFDTQ)

5,5-Dioctyl-3,7-bis(4,4,5,5-tetramethyl-1,3,2-dioxaborolan-2-yl)-5H-dibenzo[b,d]silole (0.15 g, 0.23 mmol), M2 (0.2 g 0.23 mmol), $Pd(PPh_3)_4$(0) (0.008 g, 0.007 mmol) and Aliquat336 were placed in a Schlenk tube, purged with three nitrogen/vacuum cycles, and 2 M degassed aqueous K_2CO_3 (7 mL) and dry toluene (10 mL) were added under a nitrogen atmosphere. The mixture was placed in a microwave reactor and heated to 90 °C using 300 W of microwave power for 20 min. After the polymerization was complete, the polymer was end-capped with bromothiophene. After reaction quenching, the entire mixture was poured into methanol. The precipitate was filtered off and purified with a Soxhlet extraction in the following order: methanol, acetone and chloroform. The polymer was recovered from the chloroform fraction and precipitated into methanol. The final product was obtained after drying under vacuum. Dark violet solid (0.18 g 73%). ^{1}H NMR (400 MHz; $CDCl_3$; Me_4Si): δ = 9.56 (s, 2H), 8.88 (s, 2H), 8.47–8.17 (m), 7.88–7.49 (m), 4.49 (br, 4H), 2.14 (br, 4H), 1.59–1.21 (m), 0.96–0.82 (m). Anal. Calcd for: $C_{72}H_{88}N_2O_2S_2Si$: C, 78.21; H, 8.02; N, 2.53; O, 2.89; S, 5.80. Found: C, 76.38; H, 7.71; N, 2.55; O, 2.37; S, 6.05.

3. Results and discussion

Scheme 1 shows the chemical structure and the synthesis process. As shown in this scheme, PSiPDTQ and PSiFDTQ were polymerized through the Suzuki coupling reaction using dibenzosilole and the M1, M2. The synthesis of 11,12-bis(octyloxy)-10,13-di(thiophen-2-yl)dibenzo[a,c]phenazine exhibited an improved yield (81%) using microwave reaction (reaction time 3 h) compared to thermal reaction (reaction time: 24 h, yield: 59%). [20] The polymerization was reacted in a microwave reactor for 20 min at 90 °C using palladium catalysts (0), a 2 M potassium carbonate solution, aliquot 336 as a surfactant and toluene as a solvent. Upon completion, the polymer was end-capped with boromothiophene. The synthesized polymer was purified using a Soxhlet extractor with methanol, acetone and chloroform. The chloroform fraction was recovered. The polymerization rates of PSiPDTQ and PSiFDTQ were 56% and 73%, respectively. The polymers were dissolved with organic solvents, such as THF, chloroform, and chlorobenzene, to produce a red film through spin-coating that is both homogenous and semi-transparent.

The molecular weights and thermal properties of the synthesized polymers are shown in Table 1. Using GPC with polystyrene as the standard, the number-average molecular weights (M_n) of PSiPDTQ and PSiFDTQ were determined to be 18.6 and 16.5 kg/mol, respectively. The polydispersity indices (PDI) of PSiPDTQ and PSiFDTQ exhibited very narrow distributions of 1.98 and 2.16, respectively. According to a TGA thermal analysis, shown in Table 1, high thermal stabilities were observed at 332–338 °C (5 wt% loss). These results indicated a potential use of PSiPDTQ and PSiFDTQ in polymeric solar cells or other opto-electronic devices [4], which require high thermal stabilities at temperatures of 300 °C or higher.

Fig. 1 shows the UV–Vis spectra of the solution (10^{-5} M) and the thin film (50 nm) after spin coating. The solution maximum absorption wavelengths (λ_{max}) were 369 nm and 479 nm for PSiPDTQ and 389 nm and 503 nm for PSiFDTQ. The absorption between 300 and 400 nm is caused by the π–π^* transition of the conjugated backbone. The absorption between 450–600 nm is caused by an intramolecular charge transfer (ICT) between the donors and acceptors [14].

The maximum absorption wavelengths of the thin film (λ_{max}) occurred at 374 and 502 nm for PSiPDTQ and at 393 and 522 nm for PSiFDTQ. A 4–23 nm red-shift tendency

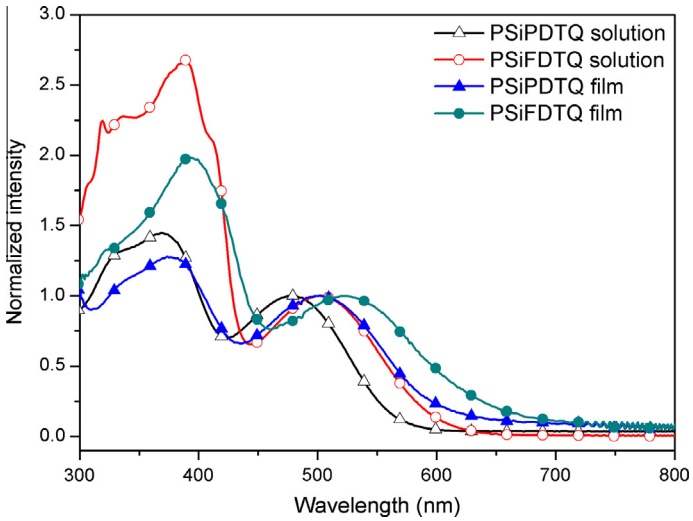

Fig. 1. Absorption spectra of polymer in solution and film.

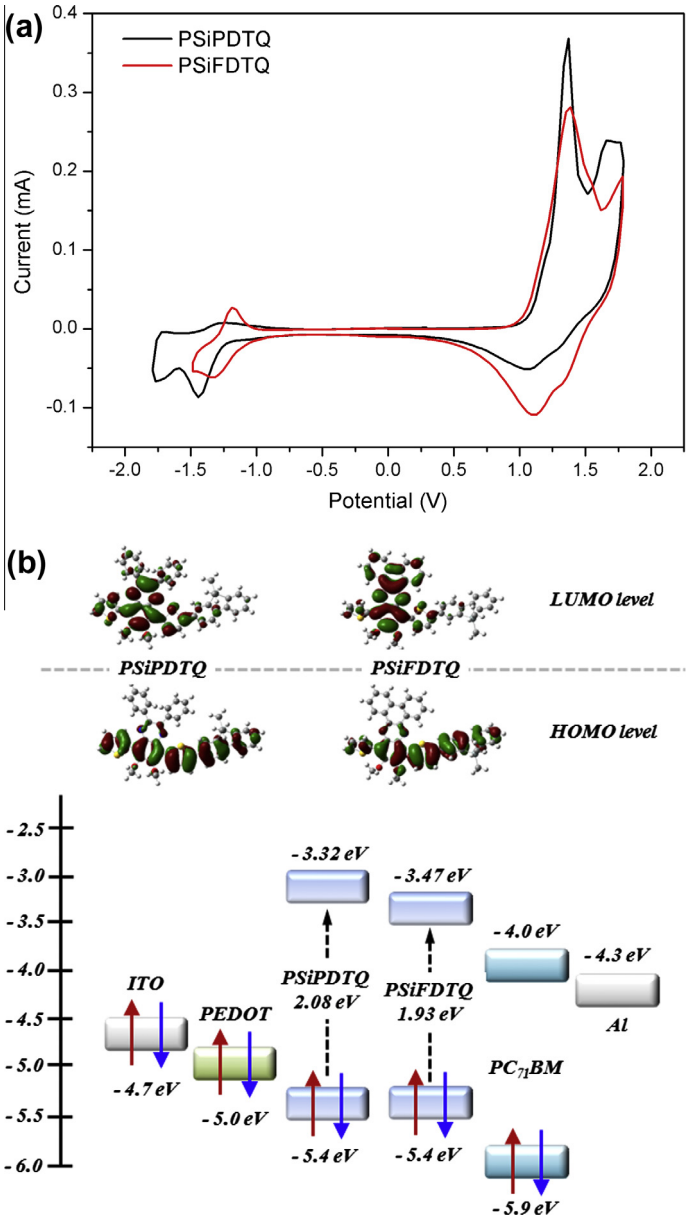

Fig. 2. (a) Cyclic voltammogram (b) DFT Gaussian simulation and band diagram of polymers (experiment level), ITO, PC71BM, Al.

Table 2
Optical and electrochemical properties of the polymers.

Polymer	Absorption, λ_{max} (nm)		E_{ox}^{onset} (V)	E_{HOMO} (eV)[c]	E_{LUMO} (eV)[d]	E_{opt} (eV)[e]
	Solution[a]	Film[b]				
PSiPDTQ	369, 479	374, 502	1.05	−5.40	−3.32	2.08
PSiFDTQ	389, 503	393, 522	1.05	−5.40	−3.47	1.93

[a] Absorption spectrum in $CHCl_3$ solution (10^{-6} M).
[b] Spin-coated thin film (50 nm).
[c] Calculated from the oxidation onset potentials under the assumption of Fc/Fc + relative Ag/AgCl (−4.8 eV below a vacuum).
[d] HOMO – Eopt.
[e] Estimated from the onset of UV–Vis absorption data of the thin film.

was observed in the thin film compared to the solution because of an effective intermolecular interaction between the polymer chains at film formation [9]. Compared with PSiPDTQ, a long-wave absorption was observed in PSiFDTQ for both the solution or the thin film, because the fused-phenyl ring of the dibenzophenazine derivative in PCzFDTQ increased the effective conjugation length by enhancing the planarity between the chain backbones, which can be explained by the ICT effects that are much stronger in PSiFDTQ than those in PSiPDTQ [9,24]. In addition, the magnitude of the absorption was higher over the wavelength range 350–450 nm in PSiFDTQ because of an increase in the π–π^* transition of the polymer backbone with the fused-phenyl ring structure [14,20]. The optical band gap energy of PSiPDTQ and PSiFDTQ calculated through the band edge were 2.08 eV and 1.93 eV, respectively.

The cyclic voltammograms of the PSiPDTQ and PSiFDTQ thin films, measured in 0.1 M tetrabutylammonium-hexafluorophosphate acetonitrile, are shown in Fig. 2(a). Table 2 contains the optical and electrochemical properties of the

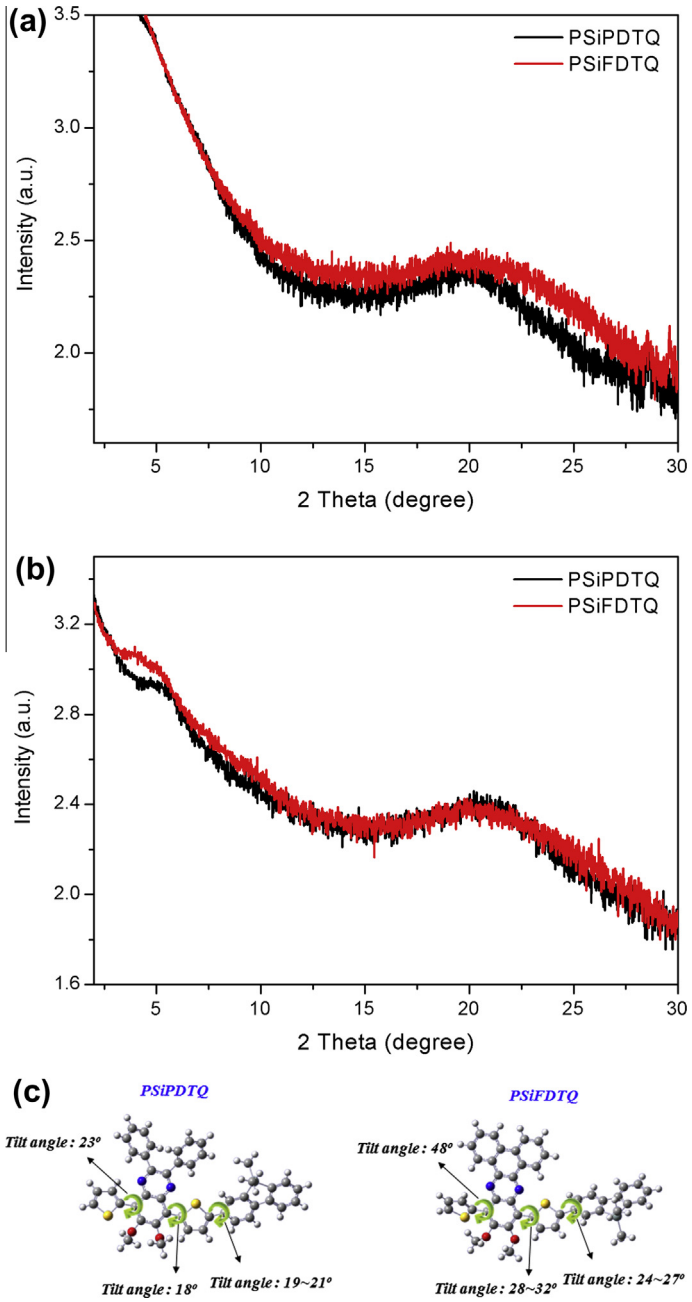

Fig. 3. (a) Out-of-plane and (b) in-plane in X-ray diffraction pattern in thin films of thermal treatment (c) tilt angle of polymer backbones by calculation of DFT Gaussian simulation.

polymers. As shown in Fig. 2(a) and Table 2, both of the oxidation (E_{ox}^{onset}) onset potential values for PSiPDTQ and PSiFDTQ were +1.05 V. The HOMO levels of PSiPDTQ and PSiFDTQ were – 5.40 eV. The LUMO levels of PSiPDTQ and PSiFDTQ, calculated from the optical band gap energy from the HOMO levels, were – 3.32 and −3.47 eV, respectively. Because all of the polymer HOMO levels are lower than the P3HT HOMO levels (4.9 eV), a relatively high air stability is expected [25]. Fig. 2(b) shows the band diagram of the energy levels obtained through CV measurement and the HOMO and LUMO distributions obtained using density functional theory (DFT) calculations in Gaussian at the B3LYP/6-31G* level. For the distribution of electrons in the LUMO level, in particular, the fused-phenyl ring of PSiFDTQ exhibited a higher electron distribution than the phenyl ring of PSiPDTQ, because the fused-phenyl ring transports electrons with a higher conjugation length than the separated-phenyl ring. As shown in the HOMO and LUMO distributions of the polymers, the LUMO orbitals of PSiPDTQ was partially located on the donor dibenzosilole derivative, which suggests an incomplete ICT effect. In contrast, the LUMO orbitals of PSiFDTQ were located primarily on the acceptor quinoxaline derivative, which suggests a strong ICT effect [26]. This result was confirmed by the aforementioned UV–Vis absorption measurement results (Fig. 1).

As shown in Fig. 2(b), among the polymers studied, the lowest difference of the LUMO levels was 0.53 eV between PSiFDTQ (−3.47 eV) and $PC_{71}BM$ (−4.0 eV), indicating that an effective electron transport is expected between PSiFDTQ and $PC_{71}BM$ [27].

Fig. 3(a) and (b) shows X-ray diffraction measurements of the film used to analyze the ordering structure of the obtained polymers. The out-of-plane peak, observed in all diffraction patterns with a highly ordered lamellar polymeric structure, was not observed. In the (0 1 0) crystal plane related to π–π stacking, a broad diffraction peak for PSiPDTQ and PSiFDTQ were detected at approximately 19.8° and 20.3°, respectively. Using the calculation ($\lambda = 2d\sin\theta$), the

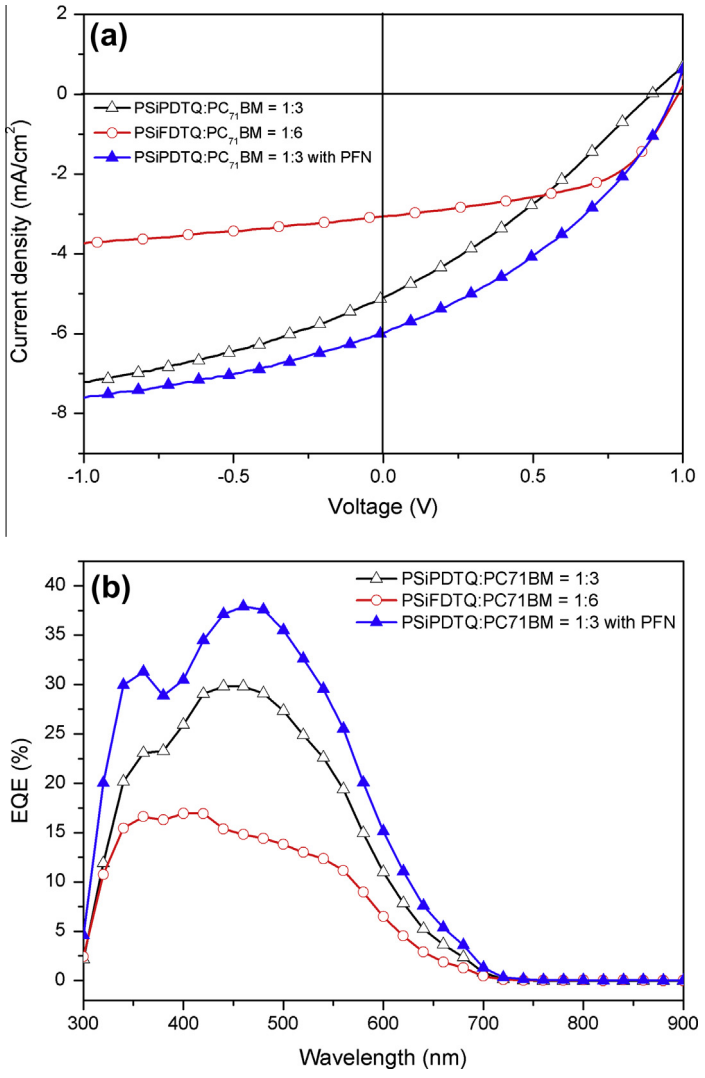

Fig. 4. (a) *J–V* characteristics and (b) EQE spectra of the BHJ solar cells with the device.

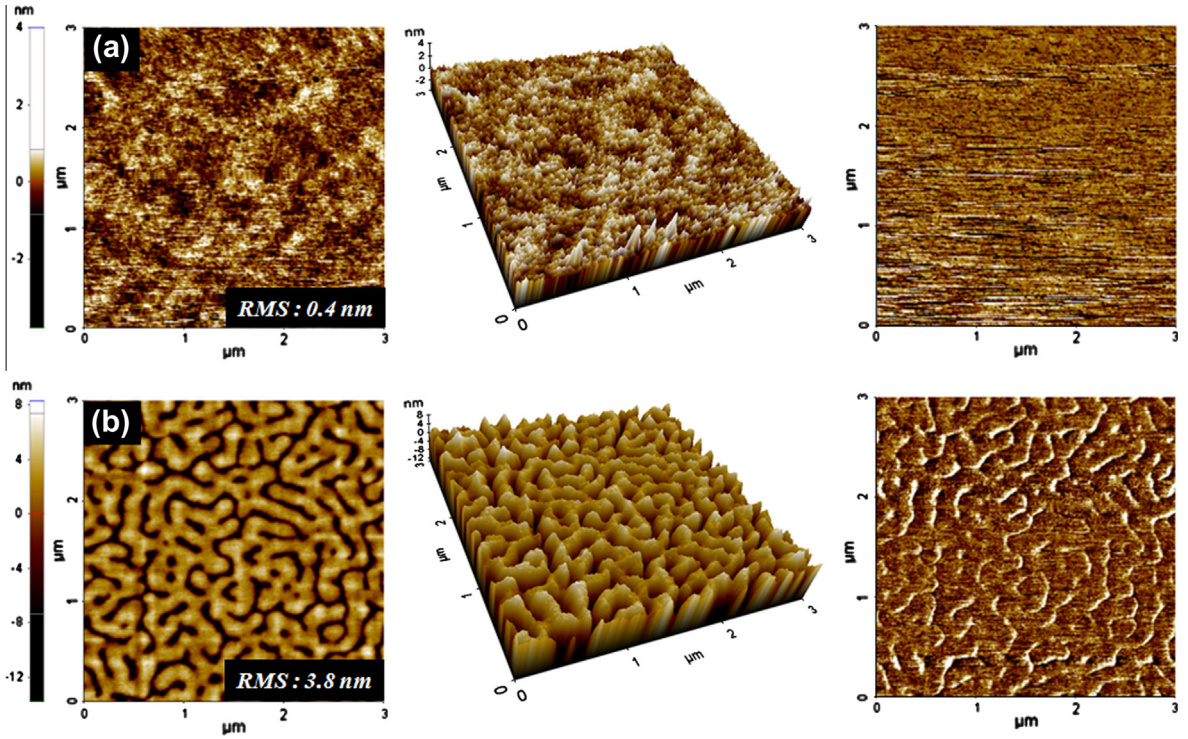

Fig. 5. Topographic AFM images of (a) PSiPDTQ: $PC_{71}BM$ 1:3 (3×3 μm^2) (b) PSiFDTQ:$PC_{71}BM$ 1:6 (3×3 μm^2).

π–π stacking distances (d_π) of PSiPDTQ and PSiFDTQ were 4.4 Å and 4.3 Å, respectively, indicating that the π–π stacking was more effective in PSiFDTQ than in PSiPDTQ. These results are similar to the benzene–thiophene aromatic system polymers that have exhibited good performance in OPVs [24].

According to a comparative analysis of the tilt angle through DFT calculations, as shown in Fig. 3(c), the tilt angle of the dibenzosilole-thiophene linkage was 28°. The thiophene–quinoxaline of PSiPDTQ and thiophene-dibenzophenazine of PSiFDTQ were 19° and 47°, respectively. In terms of the tilt angle, PSiFDTQ was greater than PSiPDTQ. However, an effective π–π stacking is enabled in PSiFDTQ because the fused-phenyl ring (tilt angle: 0°) has strong planarity properties between the chain backbones. As shown in the XRD measurement in Fig. 3, PSiFDTQ had a shorter π–π stacking distance than PSiPDTQ. A high FF is expected occur in the PSiFDTQ-containing OPVs due to the close π–π stacking of PSiFDTQ with its planarity properties.

Fig. 4(a) and Table 3 show the results of the evaluation of the characteristics of the OPV devices. Each of the devices were structured as follows: ITO (170 nm)/PEDOT:PSS (40 nm)/active layer (50 nm)/Al (100 nm). The active layer had an optimized blending ratio obtained by dissolving the polymer and $PC_{71}BM$ in chlorobenzene (CB) and 1 8-diiodooctane (DIO) with a concentration of approximately 0.5–1 wt%. For PSiPDTQ with a 1:3 ratio of $PC_{71}BM$ (50 nm in thickness), the open-circuit voltage (V_{OC}), short-circuit current (J_{SC}), fill factor (FF) and PCE were 0.89 V, 5.1 mA/cm^2, 30.2% and 1.4%, respectively. At a PSiFDTQ and $PC_{71}BM$ ratio of 1:6, the values of V_{OC}, J_{SC}, FF and PCE were 0.98 V, 3.0 mA/cm^2, 52.8% and 1.6%, respectively. While V_{OC} and J_{SC} were similar, the value of FF for PSiFDTQ increased by 74% compared to PSiPDTQ. As supported by the XRD data in Fig. 4, this increase was caused by the effects of the backbone planarity of the polymers. In other words, the effective π–π stacking found in PSiFDTQ with a high coplanarity increases the FF. Both of the synthesized polymers exhibited greater open circuit voltage values than P3HT (V_{oc} = 0.5–0.6) when used in OPVs, because of the lower HOMO levels [25]. Moreover, both of the synthesized polymers exhibited greater open circuit voltage values and fill factor than polymers using carbazole derivative (V_{OC} = ~0.85, FF = ~44.9) [20]. In other words, the polymers consisting dibenzosilole derivative show superior properties than the polymers consisting carbazole or fluorene derivative due to planarity and interaction of silicon atom [8,23].

Recently, a number of studies aimed at improving the performance of OPV devices using poly [(9,9-bis(30-(N,N-dimethylamino)propyl)-2,7-fluorene)-alt-2,7-(9,9-dioctylfluorene)] (PFN), because PFN improves the interfacial adhesion and electron transport between the active layers and the cathodes [28]. Thus, we fabricated the devices introducing PFN, and the results are summarized Fig. 4(a) and Table 3. For a device with the structure of ITO/PEDOT:PSS/active layer (PSiPDTQ:$PC_{71}BM$ = 1:3)/PFN/Al, the values of V_{OC}, J_{SC}, FF, and PCE were 0.95 V, 6.0 mA/cm^2, 36.6%, and 2.1%, respectively. The device with PFN exhibited the best performance, with improved J_{SC} and FF compared with the device without PFN, because the PFN interlayer improved the electron transport between the active layers and the Al electrode. On the other hand, for a device with the structure of ITO/PEDOT:PSS/active layer

Table 3
Photovoltaic performance of the BHJ solar cells with the device.

Active layer (w/w)		Weight ratio (P:A, w/w)	V_{OC} (V)	J_{SC} (mA/cm^2)	FF (%)	PCE (%)
Polymer (P)	Acceptor (A)					
PSiPDTQ	$PC_{71}BM$	1:3	0.89	5.1	30.2	1.4
		1:3[a]	0.95	6.0	36.6	2.1
PSiFDTQ	$PC_{71}BM$	1:6	0.98	3.0	52.8	1.6

[a] Device structure: ITO/PEDOT:PSS/blend film/PFN/Al.

(PSiFDTQ:$PC_{71}BM$ = 1:6)/PFN/Al, almost no photovoltaic response was observed. This result can be because interfacial adhesion between the blended film layer (PSiFDTQ:$PC_{71}BM$ = 1:6) and the PFN layer is poor.

To verify the accuracy of the device measurements, the External Quantum Efficiency (EQE) was measured, and the EQE curve for a device with the $PC_{71}BM$ blend is shown in Fig. 4(b). In the EQE curve, photons were primarily absorbed in the polymer phase, as the EQE spectrum correlated with the absorption spectrum of the relevant polymer [29]. As shown in Fig. 4(b), the EQE curve was similar to the UV–Vis spectra curve in Fig. 1. For PSiPDTQ, the short-circuit current density obtained from the EQE against $PC_{71}BM$ (1:3 ratio) was 3.4 mA/cm^2. For PSiFDTQ, the theoretical short-circuit current density obtained from the EQE against $PC_{71}BM$ (1:6 ratio) was 1.9 mA/cm^2. Although there were slight differences, the results are similar to the device performance measured at the AM 1.5 conditions.

The AFM of the polymer/PCBM blend films are shown in Fig. 5. As observed in Fig. 5(a), a smooth morphology appeared when PSiPDTQ and $PC_{71}BM$ were blended in a 1:3 ratio. Compared with PSiPDTQ, a large-phase separation was observed when PSiFDTQ and $PC_{71}BM$ were mixed at a 1:6 ratio, as shown in Fig. 5(b). In addition, macro p–n channels were formed. The large-phase separation produces a low photocurrent by reducing the charge separation and increasing the exciton diffusion length and the recombination of electric charges [30]. Thus, the lowest photocurrent (3.0 mA/cm^2) was observed for a PSiFDTQ/$PC_{71}BM$ ratio of 1:6. However, the FF improved by 74% due to the superior π–π stacking coplanarity. As a result, the PSiFDTQ OPV devices exhibited a relatively higher efficiency than the PSiPDTQ OPV devices for the same device structure.

4. Conclusions

In this study, two new acceptor units, in which octyloxy with a high solubility was introduced, have been synthesized. In addition, D–A type polymers, PSiPDTQ and PSiFDTQ, which accepted benzosilole derivatives as a donor, were polymerized. Both PSiPDTQ and PSiFDTQ exhibited high solubility and high thermal stability. According to XRD measurements, the π–π stacking distance (d_π) of PSiPDTQ and PSiFDTQ were 4.4 Å and 4.3 Å, respectively. With a large-phase separation, the J_{SC} of OPV devices with PCzFDTQ was lower than those with PCzPDTQ. On the other hand, with the superior coplanarity of the fused phenyl rings, the FF of the PSiFDTQ OPV device was 74% higher than that of the PSiPDTQ device.

Acknowledgements

This research was supported by a grant from the Fundamental R&D Program for Core Technology of Materials funded by the Ministry of Knowledge Economy, Republic of Korea (10037203). This work was supported by the National Research Foundation of Korea Grant funded by the Korean Government (MEST) (NRF-2009-C1AAA001-2009-0093526).

References

[1] Friend RH, Gymer RW, Holmes AB, Burroughes JH, Marks RN, Taliani C, et al. Electroluminescence in conjugated polymers. Nature 1999;397(6715):121–8.
[2] Lu W, Kuwabara J, Kanbara T. Polycondensation of dibromofluorene analogues with tetrafluorobenzene via direct arylation. Macromolecules 2011;44(6):1252–5.
[3] Song HJ, Lee JY, Song IS, Moon DK, Haw JR. Synthesis and electroluminescence properties of fluorene–anthracene based copolymers for blue and white emitting diodes. J Ind Eng Chem 2011;17(2):352–7.
[4] Song HJ, Kim DH, Lee TH, Moon DK. Emission color tuning of copolymers containing polyfluorene, benzothiadiazole, porphyrin derivatives. Eur Polym J 2012;48(8):1485–94.
[5] Iwan A, Palewicz M, Chuchmała A, Gorecki L, Sikora A, Mazurek B, et al. Opto(electrical) properties of new aromatic polyazomethines with fluorene moieties in the main chain for polymeric photovoltaic devices. Synth Met 2012;162(1–2):143–53.
[6] Lee JY, Song HJ, Lee SM, Lee JH, Moon DK. Synthesis and investigation of photovoltaic properties for polymer semiconductors based on porphyrin compounds as light-harvesting units. Eur Polym J 2011;47(8):1686–93.
[7] Xiang N, Liu Y, Zhou W, Huang H, Guo X, Tan Z, et al. Synthesis and characterization of porphyrin–terthiophene and oligothiophene p-conjugated copolymers for polymer solar cells. Euro Polym J 2010;46(5):1084–92.
[8] Chen H-Y, Hou J, Hayden AE, Yang H, Houk KN, Yang Y. Silicon atom substitution enhances interchain packing in a thiophene-based polymer system. Adv Mater 2010;22(3):371–5.
[9] Subramaniyan S, Xin H, Kim FS, Shoaee S, Durrant JR, Jenekhe SA. Effects of side chains on thiazolothiazole-based copolymer semiconductors for high performance solar cells. Adv Energy Mater 2011;1(5):854–60.
[10] Li Y. Molecular design of photovoltaic materials for polymer solar cells: toward suitable electronic energy levels and broad absorption. Acc Chem Res 2012;45(5):723–33.
[11] Huo L, Zhang S, Guo X, Xu F, Li Y, Hou J. Replacing alkoxy groups with alkylthienyl groups: a feasible approach to improve the properties of photovoltaic polymers. Angew Chem Int Ed 2011;50(41):9697–702.
[12] Yamamoto T, Kokubo H, Kobashi M, Sakai Y. Alignment and field-effect transistor behavior of an alternative π-conjugated copolymer of thiophene and 4-alkylthiazole. Chem Mater 2004;16(23):4616–8.
[13] Yasuda T, Sakai Y, Aramaki S, Yamamoto T. New coplanar (ABA)n-type Donor–Acceptor π-conjugated copolymers constituted of alkylthiophene (Unit A) and pyridazine (Unit B): synthesis using hexamethylditin, self-organized solid structure, and optical and electrochemical properties of the copolymers. Chem Mater 2005;17(24):6060–8.
[14] Lee Y, Nam YM, Jo WH. Enhanced device performance of polymer solar cells by planarization of quinoxaline derivative in a low-bandgap polymer. J Mater Chem 2011;21(24):8583–90.
[15] Blouin N, Michaud A, Gendron D, Wakim S, Blair E, Neagu-Plesu R, et al. Toward a rational design of poly(2,7-carbazole) derivatives for solar cells. J Am Chem Soc 2007;130(2):732–42.
[16] Huo L, Tan Za, Zhou Y, Zhou E, Han M, Li Y. Poly(quinoxaline vinylene) with conjugated phenylenevinylene side chain: a potential

polymer acceptor with broad absorption band. Macromol Chem Phys 2007;208(12):1294–300.
[17] Huo L, Tan Za, Wang X, Zhou Y, Han M, Li Y. Novel two-dimensional donor–acceptor conjugated polymers containing quinoxaline units: synthesis, characterization, and photovoltaic properties. J Polym Sci: Polym Chem 2008;46(12):4038–49.
[18] Huang Y, Guo X, Liu F, Huo L, Chen Y, Russell TP, et al. Improving the ordering and photovoltaic properties by extending π–conjugated area of electron-donating units in polymers with D–A structure. Adv Mater 2012;24(25):3383–9.
[19] Zhang Y, Zou J, Yip H-L, Chen K-S, Zeigler DF, Sun Y, et al. Indacenodithiophene and quinoxaline-based conjugated polymers for highly efficient polymer solar cells. Chem Mater 2011;23(9):2289–91.
[20] Song HJ, Lee TH, Han MH, Lee JY, Moon DK. Synthesis of donor–acceptor polymers through control of the chemical structure: improvement of PCE by planar structure of polymer backbones. Polymer 2013;54(3):1072–9.
[21] Boudreault P-LT, Michaud A, Leclerc M. A new poly(2,7-dibenzosilole) derivative in polymer solar cells. Macromol Rapid Commun 2007;28(22):2176–9.
[22] Chan KL, McKiernan MJ, Towns CR, Holmes AB. Poly(2,7-Dibenzosilole): a blue light emitting polymer. J Am Chem Soc 2005;127(21):7662–3.
[23] Lu G, Usta H, Risko C, Wang L, Facchetti A, Ratner MA, et al. Synthesis, characterization, and transistor response of semiconducting silole polymers with substantial hole mobility and air stability. Experiment and theory. J Am Chem Soc 2008;130(24):7670–85.
[24] Song H-J, Kim D-H, Lee E-J, Heo S-W, Lee J-Y, Moon D-K. Conjugated polymer consisting of quinacridone and benzothiadiazole as donor materials for organic photovoltaics: coplanar property of polymer backbone. Macromolecules 2012;45(19):7815–22.
[25] Hou J, Chen TL, Zhang S, Huo L, Sista S, Yang Y. An easy and effective method to modulate molecular energy level of poly(3-alkylthiophene) for high-Voc polymer solar cells. Macromolecules 2009;42(23):9217–9.
[26] Gao XK, Wang Y, Yang XD, Liu YQ, Qiu WF, Wu WP, et al. Dibenzotetrathiafulvalene bisimides: new building blocks for organic electronic materials. Adv Mater 2007;19(19):3037–42.
[27] Jiang J-M, Yang P-A, Hsieh T-H, Wei K-H. Crystalline low-band gap polymers comprising thiophene and 2,1,3-benzooxadiazole units for bulk heterojunction solar cells. Macromolecules 2011;44(23):9155–63.
[28] He Z, Zhong C, Huang X, Wong W-Y, Wu H, Chen L, et al. Simultaneous enhancement of open-circuit voltage, short-circuit current density, and fill factor in polymer solar cells. Adv Mater 2011;23(40):4636–43.
[29] Gadisa A, Mammo W, Andersson LM, Admassie S, Zhang F, Andersson MR, et al. A new donor–acceptor–donor polyfluorene copolymer with balanced electron and hole mobility. Adv Funct Mater 2007;17(18):3836–42.
[30] Wang E, Hou L, Wang Z, Ma Z, Hellström S, Zhuang W, et al. Side-chain architectures of 2,7-carbazole and quinoxaline-based polymers for efficient polymer solar cells. Macromolecules 2011;44(7):2067–73.